



A GEANT4 Study of a Gamma-ray Collimation Array

J A López^{*}, S S Romero González¹, O Hernández Rodríguez¹, J Holmes² and R Alarcón²

¹Physics Department, University of Texas at El Paso, El Paso, Texas, 79968 U.S.A.

²Physics Department, Arizona State University, Tempe, Arizona, 85281 U.S.A.

*Email: jorgelopez@utep.edu

ARTICLE INFORMATION

Received: October 10, 2019
Accepted: February 8, 2020
Published online: February 28, 2020

Keywords:

Proton therapy, Collimators, Gamma rays, GEANT4

ABSTRACT

Proton beam therapy uses high-energy protons to destroy cancer cells which are still uncertain about where in the body they hit. A possible way to answer this question is to detect the gamma rays produced during the irradiation and determine where in the body they are produced. This work investigates the use of collimators to determine where the proton interactions occur. GEANT4 is used to simulate the gamma production of a source interacting with a collimator. Each event simulates a number of gammas obtained as a function of the position along the detector. Repeating for different collimator configurations can thus help determine the best characteristics of a detector device.



DOI: [10.15415/jnp.202072028](https://doi.org/10.15415/jnp.202072028)

1. Introduction

Proton therapy uses a beam of protons to irradiate tissue in the treatment of cancer. Protons, being more massive, tend to have little lateral side scatter in the tissue keeping the beam narrow and focused on the tumor. Likewise, protons deposit their energy in a narrow range minimizing irradiation to other parts of the body. Calibrating the proton energy allows the beam to deliver its energy in the last few millimeters of the particle's range, i.e. in the Bragg peak [1]; Figure 1A shows a typical spread-out Bragg peak (SOBP) where it is compared to the radiation produced by an X-ray beam [2].

Proton energies are in the range of 70 to 250 MeV, adjusting the energy can focus the damage within the tumor and reducing the radiation to cells beyond the Bragg peak [3]. Usually protons of different energies are used to add Bragg peaks at different depths and treat an entire tumor; the tissue in front and behind the tumor does not receive much of a dose. In spite of this theoretical accuracy, it is hard to estimate where the energy being deposited during the irradiation. Since it is impossible to perform in situ inspections during the irradiation, it is necessary to rely on indirect observations.

Protons interact by inelastic Coulomb interaction with an atomic nucleus, deflection of proton trajectory by repulsive Coulomb elastic scattering with a nucleus, or by a direct collision with a nucleus removing a proton

or neutron while creating a gamma ray as illustrated in Figure 1B. Gamma rays, in turn, interact with matter in a variety of ways (Mössbauer Effect, Coherent Scattering, Pair Production, Photoelectric Effect and Compton Effect, see e. g. [4, 5]), but many will just fly through the body without interacting. By detecting those non-interacting gammas it is possible to determine the location of the source and, thus, the area where the irradiation is taking place.

At a difference with optical light, gamma rays (and X-rays) cannot be focused to produce images and, at best, one can only filter the beams with collimators to produce parallel rays which can be used to determine the main direction of a burst and the possible location of the source. Collimators filter gamma rays allowing only those parallel to the collimator to go through. Here we study the design collimators need to have to determine the directionality of gamma rays produced in proton therapy.

2. Gamma Ray Production in Proton Therapy

Proton therapy involves electrons, protons, neutrons and X rays and gamma rays, besides neutrinos, positrons, and lower electromagnetic radiation (microwave and radio waves). Protons can interact with atomic nuclei and produce gamma rays in several manners. Identifying nuclei as A, B, C, etc. excited nuclei as A*, B*, etc., protons as p, and gamma rays as γ , these interactions are:

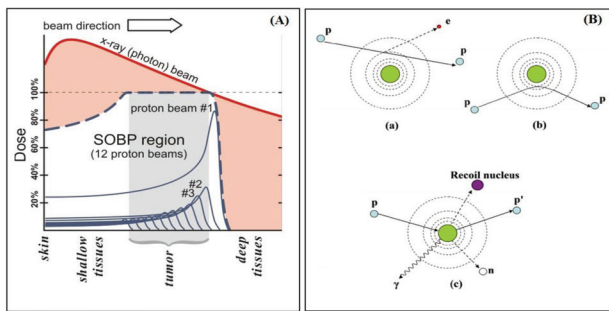


Figure 1: (A) Spread of X-ray radiation compared to proton radiation. The spread-out Bragg peak (SOBP) is actually produced by several Bragg peaks (blue lines) at different energies [2]. (B) Proton interaction mechanisms: (a) proton-electron interactions, (b) deflection of proton by the nucleus Coulomb field, (c) proton-nucleus collision [4]

- A) Radiative capture: $p + A \rightarrow B^* \rightarrow B + \gamma$, such as $p + {}^{27}\text{Al} \rightarrow {}^{28}\text{Si} + \gamma$.
- B) Inelastic scattering: $p + A \rightarrow A^* \rightarrow A + \gamma$, such as $p + {}^{27}\text{Al} \rightarrow p + {}^{27}\text{Al} + \gamma$.
- C) Rearrangement collisions: $p + A \rightarrow C^* \rightarrow C + \gamma$ such as $p + {}^{27}\text{Al} \rightarrow {}^4\text{He} + {}^{24}\text{Mg} + \gamma$.

The gamma rays are emitted with energies in the few MeVs. The proton-nucleus interactions produce gammas by bremsstrahlung and, at some energies, by gamma rays at resonance energies (ER) and the gamma yield peak is known as “Lewis Peak”. Table 1 lists a few proton-induced reactions and their characteristic gamma- rays produced.

3. GEANT4 Simulation

Geant4 is a Monte Carlo platform designed by CERN to do simulations of particle interactions [7]. A Geant4 simulation consists of a source of particles or electromagnetic radiation, a medium with a target, a detection system, and software for the analysis of the data produced. In each simulation the type of particles, their directions and energies must be specified along with the composition of the medium and the target (a type of particles, shape, structured materials, etc.), and a detection system.

The simulation is a series of “events” in which a gamma ray is produced and sent towards a chamber in a given direction and at some energy. Although the gamma ray can interact with the medium we ignore all non-wanted interactions to save computer time and allow rays to travel unperturbed. Outside the medium producing the gamma rays a collimator with some physical characteristics is situated to capture the gamma ray. In the end, the data produced consists of the energy and direction of gamma rays that manage to reach the collimator. The final step of the

simulation is the collection of information produced and its analysis done through CERN’s graphical interface ROOT.

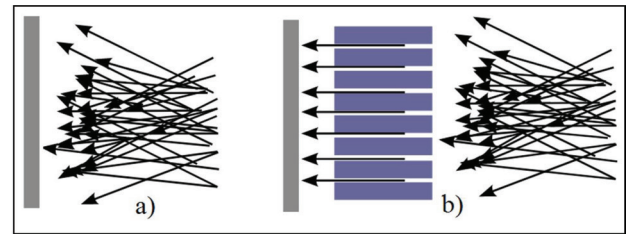


Figure 2: Beam of gamma rays with and without a collimator. The gammas are recorded on the left plates [8].

The gammas are produced in all directions (radial source) and collimated toward the detector with parallel collimating plates. Due to the small wavelength of the gamma rays the collimator does not use mirrors and lenses but simply plates of hard materials, such as lead or tungsten, here the collimator simply blocks rays that are not of our interest, and aligns those in a preferential direction. The optimization of the collimator reduces then to a study of the spacing of the plates of the collimator. Figure 2 illustrates the role of the collimator on a beam of gamma rays [8].

Table 1: Characteristic gamma ray energies in proton-induced reactions [6].

Element	Reaction	Er (keV)	Gamma ray energy (MeV)
Li	${}^7\text{Li}(p,\gamma){}^8\text{Be}$	441.4	17.7, 14.7
B	${}^{11}\text{B}(p,\gamma){}^{12}\text{C}$	163	4.43
C	${}^{13}\text{C}(p,\gamma){}^{14}\text{N}$	1748	9.17
N	${}^{14}\text{N}(p,\gamma){}^{15}\text{O}$	1059	8.3, 5.2, 3.0
	${}^{15}\text{N}(p,\gamma){}^{16}\text{C}$	429	17.7, 14.7
O	${}^{18}\text{O}(p,\gamma){}^{19}\text{F}$	1167	6.3, 2.6
F	${}^{19}\text{F}(p,\gamma){}^{20}\text{Ne}$	340.5	6.1
Na	${}^{23}\text{Na}(p,\gamma){}^{24}\text{Mg}$	1011	1.63

3.1 Collimator

The collimator is made of parallel lead plates with dimensions of 20 cm (Y component) by 20 cm (Z component), 2.2 mm of thickness and 4 mm of pitch (spacing) initially. Behind the collimator is a sensitive detector of 40 cm long (X component) by 20 cm (Y component) by 20 cm (Z component) and filled with water (water phantom). Figure 3 illustrates the collimator-detector arrangement (left) and a typical geometry of the collimation of gamma-rays produced by a single radial source. The black bars represent the collimator, the black dot at the bottom is the gamma-ray source, and the thin lines are gamma-ray trajectories. The radial source is

located at (0,0, Z). The red triangle represents the maximum angle of capture, obtained in the case where the source is just outside the collimator (next to the human body). The source was placed at a variable distance in the Z direction to optimize the capture of gamma-rays. The simulated source was a randomly radial at (0,0, Z).

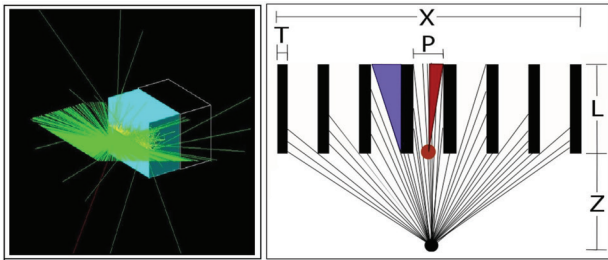


Figure 3: Left panel: geometrical arrangement of the collimator (blue blades), the water phantom detector (transparent box), and gamma rays (green). Right panel: collimation of gamma-rays produced by a single radial source next to the collimator (red dot) and at a distance Z away (black dot); the triangles denote the different pitch casted by the two sources.

The default values for the simulation are initial position at Z cm between the collimator and the source, the layers of the collimator are made of lead with geometry of 20 cm long by 20 cm height with thickness T, and the spacing (pitch, P) between each lead plate is measured from center to center of each plate. The combinations of thickness, pitch, gamma ray energy, and source location Z investigated were: T = 1, 2, 3 mm; P = 3, 4, 5, 6 mm; E = 2, 5 MeV; Z = 0, 10, 20, 40 and 80 cm. In total 120 cases were each simulated 1000 times (i.e. 1000 gamma rays).

3.2 Analysis

The goodness of the detector will be determined by the noise-to-signal ratio, which will be calculated in terms of the length of the detector, the number of bins and the so-called total signal. The length L of the collimator will be partitioned into 4000 bins, which, for the detector of 40 cm long, gives a step of 0.01cm/bin. The contrast noise-ratio (also known as signal-to-noise ratio) effectively compares the signal strength to the level of the noise ($\sqrt{\sigma}$) in the measurement [9], and it is defined as:

$$CNR = \frac{\int_{-x_0/2}^{x_0/2} Count dx}{\sqrt{\int_{-L/2}^{L/2} Count dx}} \quad (2)$$

4. Results and Conclusions

Figure 4 shows characteristic results of the gamma rays captured. As it can be seen, depending on the simulation parameters, the gamma rays pile up in various peaks; in the upcoming analyses the data collected in the central peak will be labelled as “Area 1”, those of the adjacent secondary peaks will be “Area 2”, and so on.

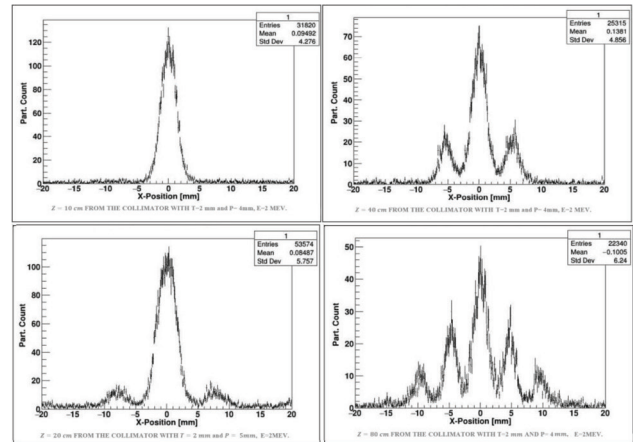


Figure 4: Gamma ray count for four different values of blade thickness, gamma ray energies and source location (and pitch).

Figure 5 shows the behavior of CNR as a function of the distance between the source and the collimator (Z from 0 to 80 cm); the data are divided according to the respective areas of the detector in which they were detected. Figure 6 shows the same as Figure 5 for the case of E = 5 MeV.

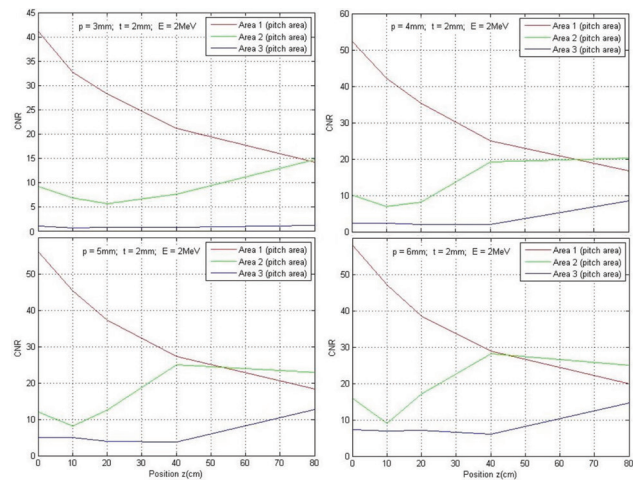


Figure 5: Behavior of CNR as a function of the distance between the source and the collimator for the cases of T = 2 mm, E = 2 MeV and pitch P = 3, 4, 5 and 6 mm.

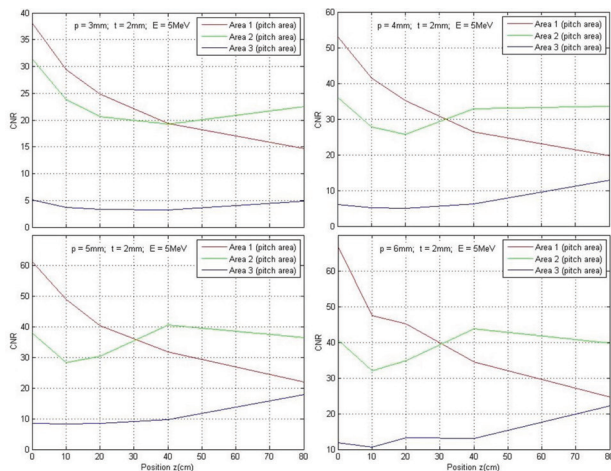


Figure 6: Same as Figure 5 for $E = 5$ MeV.

The results indicate that the data collected in the first zone in general tends to decrease as the source moves away from the collimator, while the third zone has a generally tendency to grow. This change of behavior can certainly be used to pinpoint the distance at which the source is located. For instance, one can imagine moving the collimator along the surface of the body being irradiated until a zone one signal is well detected, followed then by a displacement of the collimator perpendicular to the body until, say, a 3rd zone signal grows to a similar magnitude as in the 1st zone indicating that the source is about 80 cm away from the collimator. Likewise other comparisons between the 1st and 2nd zones could yield similar information. It must be noted that there are deviations from these results at larger values of pitch, for instance, for $P=4$ mm ($T=1$ mm, $E=2$ MeV), $P=6$ mm ($T=2$ mm, $E=5$ MeV, $Z=10$ cm to 40 cm), and $P=8$ mm ($T=2$ mm, $E=2$ MeV at $Z=40$ cm).

In summary, this exploratory study demonstrates that there is a lot of potential in the use of collimators to determine the location of the source of gamma rays.

5. Innovations and Contributions

The main innovation and contribution of this article is to introduce a way to visualize the impact zone of protons in proton therapy by means of the use of collimators.

Acknowledgements

J.A.L. acknowledges support from UTEP's BUILDING SCHOLARS Program. This work is part of the M.S. thesis of S. Romero Gonzalez [10].

References

- [1] K. A. Camphausen, R. C. Lawrence, (2009). "Principles of Radiation Therapy". In R. Pazdur, L. D. Wagman, K. A. Camphausen, W. J. Hoskins, (eds.) Cancer Management: A Multidisciplinary Approach. 11th ed., Cmp. United Business Media. ISBN-13: 978-1891483622.
- [2] W. P. Levin, H. Kooy, J. S.Loeffler, T. F., DeLaney, Proton Beam Therapy, British Journal of Cancer **93**, 849 (2005). <https://doi.org/10.1038/sj.bjc.6602754>
- [3] James Metz, (2006). "Differences Between Protons and X-rays". Abramson Cancer Center of the University of Pennsylvania. <http://www.oncolink.org/treatment/article.cfm?c=9&cs=70&id=210>. Accessed 4 February 2018.
- [4] W. D. Newhauser and R. Zhang, Phys. Med. Biol. **60**, R155 (2015). <https://doi.org/10.1088/0031-9155/60/8/R155>
- [5] Basics physics of nuclear medicine/interaction of radiation with matter. From https://en.wikibooks.org/wiki/Basic_Physics_of_Nuclear_Medicine/Interaction_of_Radiation_with_Matter. Accessed 15/9/2019
- [6] M. Chiari, Joint ICTP-IAEA Workshop on Nuclear Data for Analytical Applications. (2013) <http://indico.ictp.it/event/a12218/session/23/contribution/14/material/0/0.pdf>. Accessed 15 October 2019.
- [7] Geant4 official website. <http://geant4.cern.ch/support/introductionToGeant4.shtml>. Accessed 1 February 2018.
- [8] Fiber Optical Networking. <http://www.fiber-optical-networking.com/getting-know-fiber-collimator.html>. Accessed 9 February 2018.
- [9] J. T. Bushberg, J. A. Seibert, E. M. Leidholdt, and J. M. Boone, "The Essential Physics of Medical Imaging", Second ed., Philadelphia: Lippincott Williams & Wilkins, 2006, p. 261. ISBN 9780781780575.
- [10] S. S. Romero Gonzalez, (2018). Geant4 study of a gamma ray collimator for proton therapy. M.S. Thesis, University of Texas at El Paso. <https://digitalcommons.utep.edu/dissertations/AAI10822888/>. Accessed 10/September 2019.



Journal of Nuclear Physics, Material Sciences, Radiation and Applications

Chitkara University, Saraswati Kendra, SCO 160-161, Sector 9-C,
Chandigarh, 160009, India

Volume 7, Issue 2

February 2020

ISSN 2321-8649

Copyright: [© 2020 J A López et al.] This is an Open Access article published in Journal of Nuclear Physics, Material Sciences, Radiation and Applications (J. Nucl. Phys. Mat. Sci. Rad. A.) by Chitkara University Publications. It is published with a Creative Commons Attribution- CC-BY 4.0 International License. This license permits unrestricted use, distribution, and reproduction in any medium, provided the original author and source are credited.
